British Journal of Hospital Medicine

Br. J. Hosp. Med. (Lond) **2026**; 87(5): 54063
https://doi.org/10.31083/BJHM54063

Article

Hounsfield Unit Dynamics During CT-Guided Transthoracic Core Needle Biopsy as a Predictor of Malignant vs. Non-Malignant Thoracic Lesions

Mustafa Yeşilyurt[1,*], Buğra Kerget[2], Özlem Küçükoğlu[1], Fahri Aydın[1], Alperen Aksakal[2], Adem Karaman[1], Fatih Alper[1]

[1]Department of Radiology, Faculty of Medicine, Atatürk University, 25040 Erzurum, Turkey
[2]Department of Pulmonary Medicine, Faculty of Medicine, Atatürk University, 25040 Erzurum, Turkey
*Correspondence: drmyesilyurt@gmail.com (Mustafa Yeşilyurt)
Academic Editor: Ganesh Radhakrishna
Submitted: 3 December 2025 Revised: 15 January 2026 Accepted: 11 February 2026 Published: 22 May 2026

Abstract

Aims/Background: Hounsfield unit (HU) measurements on computed tomography (CT) offer quantitative information on tissue composition, yet their dynamic changes during CT-guided transthoracic core needle biopsy (TCNB) have not been previously investigated. This study aimed to determine whether the post-biopsy change in HU (ΔHU) at the needle tract can predict histopathological outcomes in thoracic lesions, serving as a surrogate marker of tissue viability and vascularity. **Methods**: This study retrospectively included 166 patients who underwent CT-guided TCNB between June 2023 and November 2025. Non-contrast CT images (2-mm slices) obtained immediately before and after biopsy were analyzed. Regions of interest were placed along the biopsy tract, avoiding air and necrotic components. ΔHU was calculated by subtracting pre-biopsy from post-biopsy HU values. Two radiologists independently measured HU, with excellent interobserver agreement ($\alpha = 0.849$). ΔHU values were compared across histopathological groups (malignant, necrotic, inflammatory), and diagnostic performance was assessed using receiver operating characteristic (ROC) analysis. **Results**: Malignant lesions demonstrated higher attenuation values pre-biopsy (median 32 [interquartile range (IQR) 25–40] HU) and post-biopsy (41 [35–49.25] HU) compared with necrotic (31.5 [24.5–35] HU and 25 [20–30] HU) and inflammatory lesions (27 [12–35] HU and 25 [12–37] HU), respectively ($p < 0.001$). ΔHU was positive in malignant lesions (10 [7–13] HU), negative in necrotic lesions (–3.5 [–6 to –1.25] HU), and minimal in inflammatory lesions (1 [–2 to 2] HU) ($p < 0.001$). ΔHU showed excellent discriminatory ability for malignancy (area under the curve [AUC] = 0.956), with a sensitivity of 94% and a specificity of 78%. **Conclusion**: ΔHU measurement during TCNB may serve as a quantitative biomarker with potential to differentiate malignant from necrotic or inflammatory thoracic lesions. Incorporating ΔHU may provide additional information that could enhance diagnostic confidence and guide biopsy targeting, although prospective studies are needed to confirm its impact on clinical decision-making.

Keywords: biopsy; needle; thoracic neoplasms; diagnostic imaging

1. Introduction

Computed tomography (CT)-guided percutaneous transthoracic core needle biopsy (TCNB) has become an indispensable tool in the diagnostic evaluation of thoracic masses and pulmonary nodules. This minimally invasive technique allows for precise lesion targeting under real-time tomographic guidance, enabling high diagnostic accuracy while maintaining a favorable safety profile. Reported diagnostic yields for TCNB range from 85% to 95%, depending on lesion size, location, and operator experience [1–3]. Nevertheless, despite technical advancements, non-diagnostic results and sampling errors remain a concern, particularly in heterogeneous lesions that contain necrotic, hemorrhagic, or fibrotic components [4]. These challenges underscore the importance of identifying imaging markers that reflect the underlying tissue viability and vascularity at the biopsy site. Furthermore, procedural safety relies not only on careful imaging guidance but also on thorough pre-procedural patient assessment, including evaluation of coagulation parameters and platelet counts, as abnormalities in these laboratory indices have been associated with increased risk of bleeding or other complications [5]. Being aware of potential adverse events (such as pneumothorax, hemorrhage, or hemoptysis) and knowing their incidence are essential for optimizing patient selection, minimizing procedural risk, and interpreting post-biopsy imaging changes in clinical practice. Given these challenges, quantitative imaging metrics such as CT attenuation may provide additional insight into tissue characteristics, potentially guiding biopsy targeting and predicting malignant versus non-malignant pathology.

However, recent large-scale and multicenter studies have shown that the diagnostic performance of CT-guided transthoracic biopsy may vary substantially across different institutions and patient populations. Factors such as operator experience, lesion characteristics, and institutional practice patterns have been reported to influence diag-

nostic accuracy. In a recent multicenter study, Basiri *et al*. [6] reported a diagnostic accuracy of 82.9% for CT-guided percutaneous transthoracic needle biopsy, which was lower than the rates commonly reported in single-center series. This discrepancy highlights the limitations of conventional biopsy assessment and the need for adjunct quantitative imaging-based parameters to improve diagnostic confidence.

CT attenuation, expressed in Hounsfield units (HUs), provides a quantitative measure of tissue density based on the degree of X-ray beam attenuation. HU values are defined on a relative scale, with air assigned –1000 HU, distilled water 0 HU, and dense cortical bone approximately +1000 HU [7]. The attenuation coefficient primarily depends on the physical density and effective atomic number of the tissue. Moreover, iodinated contrast media, blood volume, and perfusion markedly influence measured attenuation, a relationship demonstrated in perfusion/dynamic contrast-enhanced CT (DCE-CT) and dual-energy CT studies [8–10]. Viable, cellular, or vascularized tissues generally exhibit higher attenuation, whereas necrotic, cystic, or poorly perfused regions demonstrate lower HU values [11].

During CT-guided biopsy, both the pre-procedural scan used for needle planning and the post-biopsy scan for immediate complications provide opportunities to assess local attenuation characteristics. Mechanical disruption by the needle, micro-hemorrhages, and transient changes in perfusion can cause measurable alterations in HU at the biopsy site. However, the direction and magnitude of these attenuation changes may vary depending on lesion vascularity, internal composition, and the timing of post-procedure imaging. These variations may indirectly reflect the vascular and cellular composition of the sampled region. For example, tissues rich in viable cells and capillary networks may demonstrate a greater post-biopsy increase in attenuation due to localized hemorrhage and contrast redistribution, whereas necrotic or avascular regions may show minimal change or even decreased attenuation [12].

Despite the extensive use of CT for procedural guidance, the potential diagnostic information embedded in these subtle HU variations remains underexplored. A systematic evaluation of pre- and post-biopsy HU changes in relation to histopathological findings may provide valuable insight into tissue viability, sampling adequacy, and diagnostic yield. Understanding this relationship could improve target selection during biopsy, reduce non-diagnostic sampling, and enhance the role of imaging biomarkers in interventional radiology.

Previous studies have focused on static CT attenuation values, lesion size, or procedural factors affecting diagnostic yield and the complication rates of CT-guided transthoracic biopsy. However, dynamic changes in tissue attenuation during the biopsy itself have not been systematically evaluated. To the best of our knowledge, this is the first retrospective study to investigate pre- to post-biopsy HU changes along the needle tract as a quantitative, contrast-free, intra-procedural biomarker for predicting malignancy in thoracic lesions. Importantly, this approach was designed to be applicable in routine clinical settings where rapid on-site cytopathology evaluation is not available, aiming to support biopsy targeting and specimen adequacy assessment using readily obtainable imaging data. By analyzing attenuation change (ΔHU) rather than single time-point measurements, the present study aims to provide real-time insight into tissue viability and vascularity at the biopsy target, potentially improving sampling adequacy and diagnostic confidence without altering standard biopsy protocols.

2. Methods

2.1 Patients

A total of 201 patients who underwent CT-guided transthoracic biopsy for pulmonary or thoracic lesions in the Department of Radiology, Faculty of Medicine, Atatürk University, between June 2023 and November 2025 were retrospectively analyzed.

The study was approved by the local ethics committee of Atatürk University (approval no: 26, meeting no: 10, date: 28.11.2025) and conducted in accordance with the Declaration of Helsinki. Ethics approval was obtained prior to data analysis and manuscript preparation. Written informed consent for the biopsy procedure was obtained from all patients as part of routine clinical care. Due to the retrospective nature of the study and the use of anonymized data, the requirement for additional research-specific informed consent was waived by the ethics committee.

Patients were excluded from the study only when reliable HU measurement could not be performed. Specifically, 17 patients who demonstrated post-procedural air artifacts or dense air collections along the needle tract and 12 patients with poor image quality or severe motion artifacts were excluded. Additionally, six patients with lesions containing extensive calcification or cavitation were excluded, as these features can substantially alter CT attenuation measurements and compromise reliable HU assessment. Dense calcifications may cause beam-hardening artifacts and artificially elevated attenuation values, whereas cavitary components introduce air-tissue interfaces that result in marked partial volume effects and unstable HU measurements. Excluding such lesions was therefore necessary to ensure consistency and reproducibility of pre- and post-biopsy attenuation analysis along the needle tract. After applying these criteria, 166 patients were included in the final analysis (Fig. 1). Histopathological diagnoses were classified as malignant, necrotic, or inflammatory.

2.2 Pre-Procedural Preparation

Prior to biopsy, all patients underwent routine coagulation testing, including prothrombin time, platelet count, and bleeding time, and only those with results within normal limits were cleared for the procedure. Patients receiv-

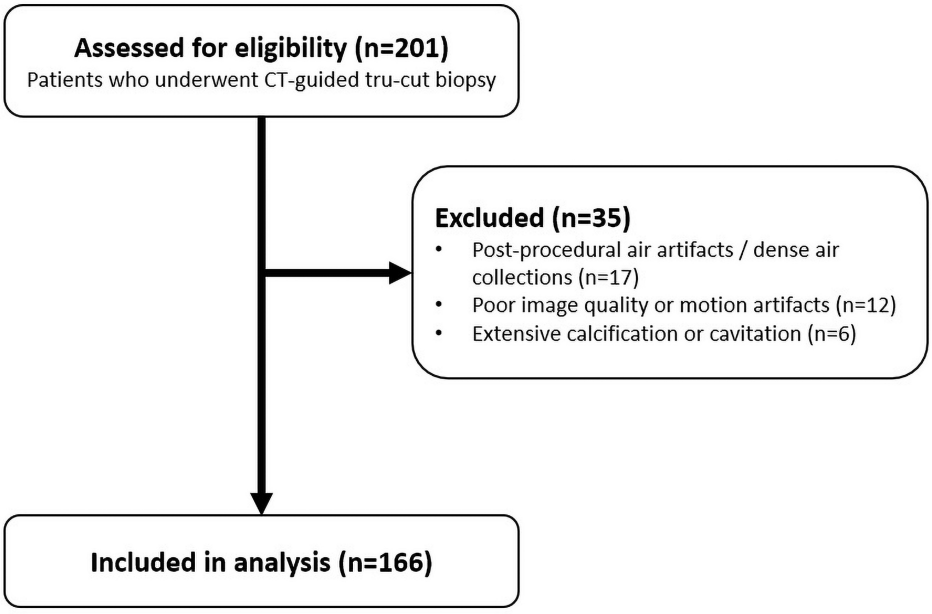

Fig. 1. Flow chart of patient selection for the study. CT, computed tomography.

ing antithrombotic therapy had their medications withheld before biopsy to minimize bleeding risk. Specifically, individuals on aspirin and/or clopidogrel underwent biopsy at least one week after discontinuation of antiplatelet therapy. Patients receiving low-molecular-weight heparin omitted their dose on the day of the biopsy.

Patients were informed about the biopsy technique, potential complications, and precautionary measures before providing written informed consent. An intravenous line was established in each patient prior to the procedure to ensure immediate venous access if needed.

2.3 Biopsy Methods

Patients were positioned supine or prone according to lesion location. All procedures were performed using a 320-row detector CT scanner (Aquilion ONE Vision; Toshiba Medical Systems Corporation, Otawara, Japan). Initial planning CT scans were obtained using standard parameters (100 kV, 120 mA, 2-mm slice thickness, and 2-mm intervals) to determine the safest needle trajectory. If pre-procedural positron emission tomography-computed tomography (PET-CT) or contrast-enhanced thoracic magnetic resonance imaging (MRI) was available, these images were evaluated to identify the most metabolically active or contrast-enhancing region of the lesion to determine the optimal biopsy target. Needle paths were planned to avoid major vessels, the heart, pulmonary bullae, and interlobar fissures, while keeping the needle as perpendicular to the pleura as possible.

During the procedure, intermittent 1-mm slice-thickness scans were used for precise needle guidance. The initial planning CT served as the pre-biopsy dataset, and a post-biopsy CT was obtained with identical parameters (2-mm slice thickness, same reconstruction kernel and window/level settings) within 1 to 3 minutes after specimen retrieval to assess complications and perform attenuation measurements. Although intra-procedural guidance scans were obtained with 1-mm slice thickness for precise needle placement, all HU measurements were consistently performed on 2-mm reconstructions to minimize partial-volume effects and ensure comparability between pre- and post-biopsy datasets. No intravenous contrast was administered for pre- or post-biopsy imaging.

After local anesthesia with 5 mL of 1% lidocaine, a 17G coaxial introducer needle was advanced into the lesion under CT guidance, followed by tissue sampling with an 18G automated cutting needle. Two to three cores (approximately 1 cm each) were obtained for histopathology, with additional samples sent for microbiological analysis when infection was suspected. The 17G coaxial system was selected to allow collection of multiple tissue samples through a single pleural puncture, thereby reducing pleural trauma and pneumothorax risk, while the 18G automated cutting needle was used to obtain adequate core specimens for histopathological evaluation without significantly increasing complication rates, as supported by previous studies [3,13].

In routine clinical practice, rapid on-site cytopathology evaluation is often unavailable due to resource limitations, as in our center. Therefore, we implemented a standardized quantitative imaging-based approach using intra-procedural attenuation measurements (pre- and post-biopsy HU) to indirectly assess biopsy targeting and specimen adequacy.

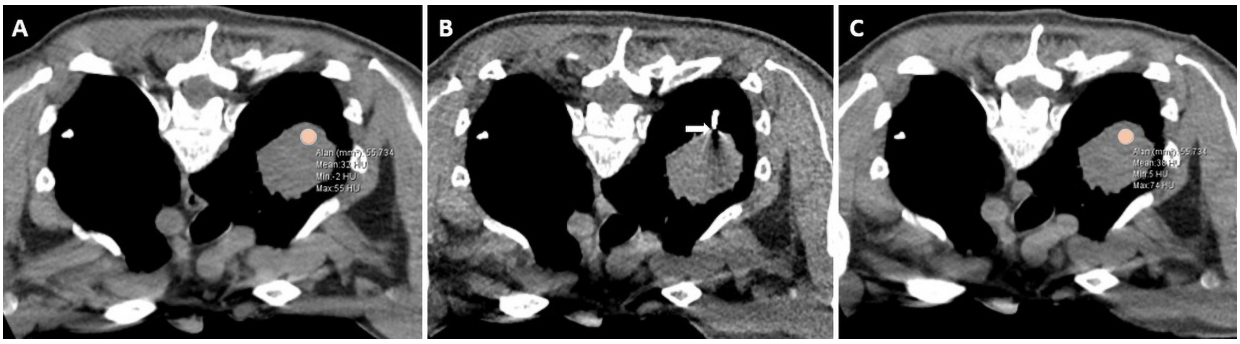

Fig. 2. Representative axial CT images obtained before (A), during (B), and after (C) CT-guided core needle biopsy of a thoracic lesion. (A) Pre-biopsy image showing the circular ROI (area = 55.7 mm^2, mean = 33 HU). (B) Intra-procedural image demonstrating coaxial needle placement within the lesion (arrow). (C) Post-biopsy image at the same slice level showing the anatomically matched ROI (area = 55.7 mm^2, mean = 38 HU). ROI, region of interest; HU, Hounsfield unit.

2.4 Image Analysis

In both pre- and post-biopsy CT scans (obtained using 2-mm slice thickness), HU measurements were performed at the exact site where the biopsy needle traversed the lesion. Circular regions of interest (ROIs) with an area of approximately 0.5–0.6 cm^2 (8–9 mm in diameter) were manually placed around the needle tract and adjacent lesion parenchyma (Fig. 2; one representative ROI shown). To ensure spatial consistency, pre- and post-biopsy measurements were obtained from the same axial slice level using identical anatomical landmarks and needle trajectory as reference. To reduce variability related to manual ROI placement, all measurements were made using a standardized approach with identical ROI size and careful positioning to avoid visible air artifacts, necrotic zones, vessels, calcifications, and beam-hardening artifacts.

The ROI size (0.5–0.6 cm^2) was deliberately selected to encompass the biopsy needle tract and adjacent lesion parenchyma while minimizing partial-volume effects and excluding surrounding aerated lung tissue. This ROI size also allowed standardized assessment of local attenuation changes across pre- and post-biopsy measurements. Similar ROI sizes have been used in prior studies assessing thoracic lesion density and reproducibility, including HU-based measurements in thoracic vascular structures [14].

Each HU measurement was performed three times, and the mean value was used for analysis. The change in attenuation ($\Delta HU = HU_{post} - HU_{pre}$) was calculated for each lesion. To minimize observer bias, HU measurements were independently performed by two radiologists (with 15 and 5 years of thoracic imaging experience, respectively), blinded to the histopathological results. Interobserver reliability was assessed using Cronbach's alpha coefficient, which demonstrated excellent agreement ($\alpha = 0.849$). Based on this high level of concordance, a consensus value (the average of both radiologists' measurements) was used for subsequent statistical analyses. Finally, HU changes were categorized according to final pathology results as malignant, necrotic, or inflammatory to analyze the degree of attenuation change across these histopathological groups.

2.5 Statistical Analysis

Statistical analyses were performed using IBM SPSS Statistics version 27.0 (IBM Corp., Armonk, NY, USA). The distribution of continuous variables was evaluated using the Shapiro-Wilk test. Data with a normal distribution were expressed as mean $\pm$ standard deviation (SD), while non-normally distributed data were presented as median (interquartile range [IQR]) values. Categorical variables were summarized as frequency and percentage. Comparisons between more than two independent groups were performed using the one-way ANOVA with *post hoc* pairwise comparisons using Bonferroni correction for normally distributed variables and the Kruskal-Wallis test with *post hoc* Dunn's test for non-normally distributed variables. Categorical variables were compared using the chi-square (χ^2) test or the Fisher–Freeman–Halton exact test with Monte Carlo simulation when appropriate. Complication subtype frequencies were presented descriptively only and were not subjected to formal subgroup comparison because of sparse cell distributions and very low expected frequencies. A two-tailed p-value < 0.05 was considered statistically significant.

Pre-biopsy HU, post-biopsy HU, and ΔHU were predefined as primary imaging variables of interest. Receiver operating characteristic (ROC) curve analysis was used to assess the diagnostic performance of these parameters in differentiating malignant from non-malignant lesions. The area under the curve (AUC) with 95% confidence interval (CI) was calculated, and the optimal ΔHU cut-off for predicting malignancy was determined using the Youden index.

There were no missing data for any of the analyzed variables. Outliers were assessed using visual inspection of boxplots and distribution analysis. However, no values were excluded, as all measurements were considered clin-

Table 1. Comparison of demographic, laboratory, clinical, and radiological data by histopathological diagnosis (n = 166).

	Malignancy (n = 120)	Necrosis (n = 25)	Inflammation (n = 21)	*p*-value	χ^2/F/H
Age (years)	67 (32–85)	66 (21–78)	58 (43–75)	0.027	7.216
Gender (male)	94 (78.3)	18 (72)	19 (90.5)	0.297	2.430
Complication (n%)	50 (41.7)	6 (24.0)	7 (33.3)	0.228	
- Hemorrhage	16 (13.3)	3 (12)			
- Hemoptysis	4 (3.3)	1 (4)	1 (4.8)		
- Pneumothorax	28 (23.3)	2 (8)	5 (23.8)		
- Hemorrhage + Pneumothorax	2 (1.7)		1 (4.8)		
Hemoglobin (g/dL)	13.70 ± 2.07	12.63 ± 1.61	13.65 ± 2.11	0.06	2.166
Platelet ($\times 10^3$/μL)	311.11 ± 105.11	341.24 ± 84.93	303.84 ± 77.69	0.19	2.061
INR	1.13 ± 0.14	1.15 ± 0.13	1.15 ± 0.20	0.57	0.373
PT (sec)	14.61 ± 1.94	14.87 ± 1.91	14.64 ± 2.24	0.66	0.377
aPTT (sec)	28.88 ± 4.32	27.74 ± 3.83	28.49 ± 3.11	0.78	0.613
Pre-TCNB HU	32 (25–40)	31.5 (24.5–35)	27 (12–35)	<0.001	8.215
Post-TCNB HU	41 (35–49.25)	25 (20–30)	25 (12–37)	<0.001	15.600
ΔHU	10 (7–13)	–3.5 (–6– –1.25)	1 (–2–2)	<0.001	83.860

Complication analysis was performed based on the presence of any complication per patient (yes/no). Individual complication types are presented descriptively. Data are presented as mean ± standard deviation (SD) for normally distributed variables and median (interquartile range [IQR]) for non-normally distributed variables. Categorical variables were compared using the Chi-square (χ^2) test or Fisher-Freeman-Halton exact test with Monte Carlo simulation where expected cell counts were less than 5. Non-normally distributed continuous variables (Age, HU values) were compared using the Kruskal-Wallis test (H statistic). INR, international normalized ratio; PT, prothrombin time; aPTT, activated partial thromboplastin time; TCNB, transthoracic core needle biopsy; HU, Hounsfield unit.

ically and technically plausible within the context of CT-guided transthoracic biopsy.

3. Results

The median age of all patients included in the study was 65 years (range: 19–85). When grouped according to TCNB findings, the median ages were 67 (32–85) years in the malignancy group, 66 (21–78) years in the necrosis group, and 58 (43–75) years in the inflammation group, showing a statistically significant difference between the groups ($p = 0.027$). In terms of gender distribution, 78.3% of the patients in the malignancy group, 72% in the necrosis group, and 90.5% in the inflammation group were male, with no statistically significant difference between the groups ($p = 0.297$). Detailed demographic, laboratory, and radiological characteristics are summarized in Table 1.

Procedure-related complications occurred in 50 patients in the malignancy group, 6 in the necrosis group, and 7 in the inflammation group, with no statistically significant difference among groups ($p = 0.228$) (Table 1). Pneumothorax was the most frequent complication, observed with 23.3% of malignant, 8% of necrotic, and 23.8% of inflammatory lesions. Hemorrhage occurred in 13.3% of malignant and 12% of necrotic lesions, while no hemorrhage was observed in the inflammatory group. Hemoptysis was noted in 3.3%, 4%, and 4.8% of cases, respectively. The coexistence of hemorrhage and pneumothorax was rare, observed only in 1.7% of malignant and 4.8% of inflammatory lesions.

There were no statistically significant differences between the groups in laboratory parameters, including hemoglobin, platelet count, and coagulation indices (international normalized ratio [INR], prothrombin time [PT], activated partial thromboplastin time [aPTT]), with $p = 0.06$, $p = 0.19$, $p = 0.57$, $p = 0.66$, and $p = 0.78$, respectively (Table 1).

Radiological attenuation (HU) values measured before and after TCNB differed significantly among the diagnostic groups, with malignant lesions showing higher pre- and post-biopsy HU and positive ΔHU compared with necrotic and inflammatory lesions ($p < 0.001$) (Table 1).

The demographic, laboratory, and radiological findings of patients diagnosed with malignancy based on TCNB results are presented in Table 2. Age did not differ significantly among histopathological subgroups ($p = 0.11$). Male predominance was observed across most histopathological subgroups, and gender distribution differed significantly among tumor types ($p = 0.015$). Procedure-related complications were seen in 7 patients with small cell carcinoma, 19 with adenocarcinoma, 13 with squamous cell carcinoma, 4 with distant metastases, 4 with neuroendocrine tumors, and 3 with lymphoma ($p = 0.641$).

No significant intergroup differences were observed among the malignant subgroups in terms of laboratory parameters, including hemoglobin, platelet count, INR, PT, and aPTT ($p = 0.09$, $p = 0.17$, $p = 0.38$, $p = 0.54$, and $p = 0.67$, respectively) (Table 2).

Pre- and post-biopsy HU values varied across subgroups, with the highest attenuation observed in small cell

Table 2. Comparison of demographic, laboratory, clinical, and radiological characteristics in patients with malignancy (n = 120), by histopathological diagnosis.

	Small cell cancer (n = 19)	Adenocarcinoma (n = 48)	Squamous cell cancer (n = 30)	Distant organ metastasis (n = 8)	Neuroendocrine tumors (n = 5)	Lymphoma (n = 8)	Large cell cancer (n = 2)	*p*-value	χ^2/F/H
Age (years)	68 (54–73)	66.5 (58–73.25)	71 (61–74)	62.5 (50.5–73.5)	65 (62.5–70.5)	59 (52.75–59.75)	71 (N/A)	0.11	10.461
Gender (male)	14 (73.7)	38 (79.2)	28 (93.3)	3 (37.5)	3 (60)	7 (87.5)	1 (50)	0.015	
Complication (n%)	7 (36.8)	19 (39.6)	13 (43.3)	4 (50.0)	4 (80.0)	3 (37.5)	0 (0.0)	0.641	
- Hemorrhage	2 (10.5)	3 (6.3)	5 (16.7)	1 (12.5)	3 (60.0)	2 (25)			
- Hemoptysis	2 (10.5)	1 (2.1)	1 (3.3)						
- Pneumothorax	2 (10.5)	15 (31.3)	6 (20)	3 (37.5)	1 (20)	1 (12.5)			
- Hemorrhage + Pneumothorax	1 (5.3)		1 (3.3)						
Hemoglobin (g/dL)	12.13 ± 1.45	13.81 ± 2.40	13.71 ± 2.21	15.05 ± 1.45	13.32 ± 0.54	14.05 ± 1.95	14.50 ± 0.56	0.09	1.521
Platelet ($\times 10^3/\mu L$)	375.21 ± 126.66	319.89 ± 109.58	296.39 ± 84.82	300.12 ± 117.11	322.00 ± 124.53	238.13 ± 49.51	198.00 ± 110.31	0.17	1.532
INR	1.17 ± 0.11	1.12 ± 0.14	1.11 ± 0.13	1.12 ± 0.23	1.15 ± 0.18	1.06 ± 0.09	1.06 ± 0.11	0.38	0.934
PT (sec)	14.9 ± 1.66	14.66 ± 1.89	14.28 ± 1.71	14.28 ± 3.29	14.92 ± 2.60	14.07 ± 0.96	13.35 ± 0.78	0.54	0.834
aPTT (sec)	28.65 ± 3.73	29.24 ± 3.81	27.49 ± 4.48	29.35 ± 6.61	28.58 ± 4.13	29.32 ± 5.38	28.90 ± 7.92	0.67	0.667
Pre-TCNB HU	43 (35–46)	30 (25–37)	28.5 (19.5–33.2)	40 (26.8–49.3)	33 (26–42)	35 (34–42.5)	40 (21–N/A)	0.002	21.011
Post-TCNB HU	47 (42–54)	41 (37–49)	35 (28–40.25)	45.5 (37.5–60.75)	40 (31–54)	45.5 (41–52.8)	51 (27–N/A)	0.001	21.590
ΔHU	11 (4–14)	10 (8–14)	8 (6–11)	9.5 (7.5–13.8)	8 (4.5–12)	7 (5.5–10)	11 (6–N/A)	0.47	0.947

Note: Data are presented as mean ± standard deviation (SD) for normally distributed variables and median (interquartile range [IQR]) for non-normally distributed variables. Categorical variables (e.g., gender, complications) were compared across subgroups using the Fisher-Freeman-Halton exact test with Monte Carlo simulation, as expected cell counts were frequently less than 5. Non-normally distributed continuous variables (Age, HU values) were compared using the Kruskal-Wallis test (H statistic). IQR could not be fully estimated in subgroups with very small sample sizes. N/A, Not applicable; INR, international normalized ratio; PT, prothrombin time; aPTT, activated partial thromboplastin time; TCNB, transthoracic core needle biopsy; HU, Hounsfield unit.

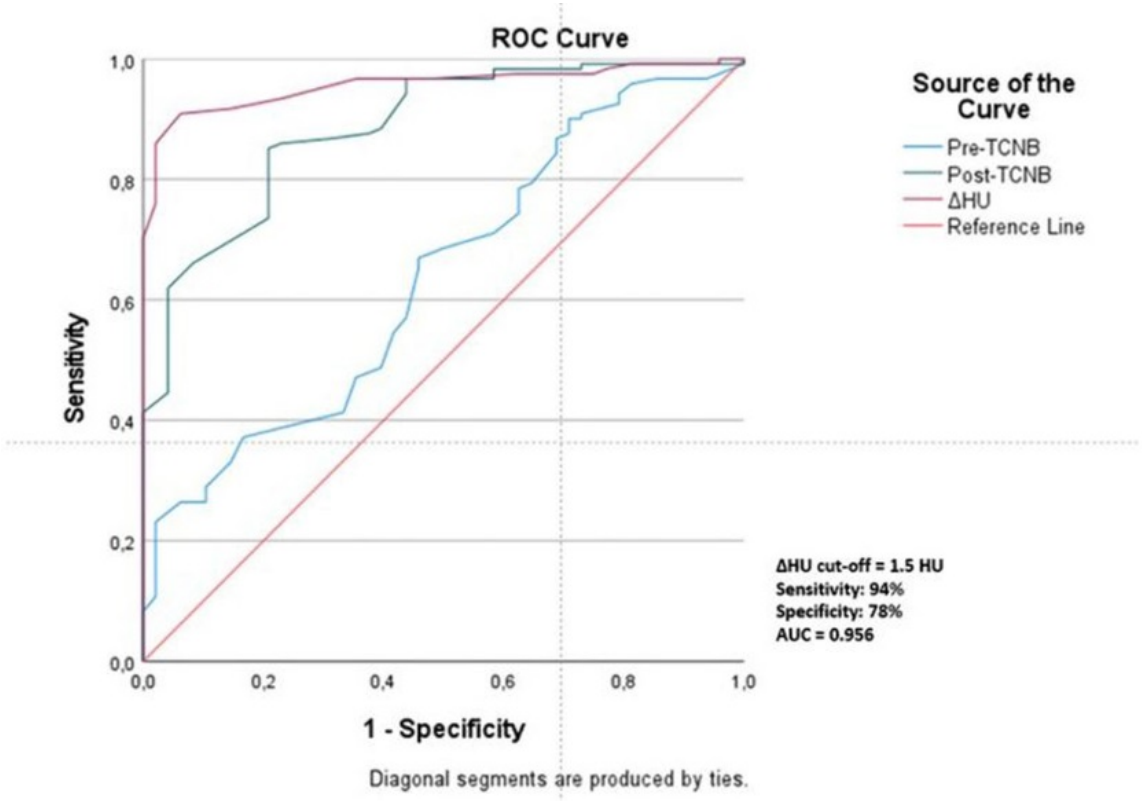

Test Result Variables	Area	Std. Error	*p*-value	Asymptotic 95% Confidence Interval	
				Lower Bound	Upper Bound
Pre-TCNB HU	0.637	0.045	0.006	0.546	0.727
Post-TCNB HU	0.886	0.026	<0.001	0.834	0.937
ΔHU	0.956	0.015	<0.001	0.927	0.986

Fig. 3. ROC curve analysis of HU before and after TCNB and HU change in patients with and without malignancy. Using a ΔHU cut-off value of 1.5 HU, sensitivity and specificity for predicting malignancy were 94% and 78%, respectively. ROC, receiver operating characteristic.

carcinoma, and the lowest in squamous cell carcinoma. ΔHU tended to be higher in small cell carcinoma and adenocarcinoma, although these differences were not statistically significant ($p = 0.47$).

The diagnostic performance of pre-biopsy HU, post-biopsy HU, and ΔHU values for differentiating malignant from non-malignant lesions was evaluated by ROC curve analysis (Fig. 3). Pre-biopsy HU showed fair discriminative ability, with an AUC of 0.637 (95% CI: 0.546–0.727, $p = 0.006$). Post-biopsy HU demonstrated higher diagnostic accuracy, with an AUC of 0.886 (95% CI: 0.834–0.937, $p < 0.001$). ΔHU exhibited the strongest diagnostic power, with an AUC of 0.956 (95% CI: 0.927–0.986, $p < 0.001$). The optimal ΔHU cut-off value was determined using the Youden index derived from ROC curve analysis. Using a ΔHU cut-off value of 1.5 HU, the model predicted malignancy with 94% sensitivity and 78% specificity.

4. Discussion

In this retrospective study, we investigated changes in attenuation (ΔHU) after CT-guided TCNB of thoracic lesions and analyzed their correlation with histopathological outcomes. Malignant lesions consistently exhibited a positive ΔHU, indicating an increase in attenuation post-biopsy, whereas necrotic lesions demonstrated a negative ΔHU and inflammatory lesions showed minimal change. These results suggest that ΔHU measurement could be used intra-procedurally to predict sample adequacy before histological confirmation, potentially reducing the need for repeat biopsies in thoracic lesions. This quantitative approach may potentially complement artificial intelligence (AI)-based imaging tools or radiomics, providing additional information in estimating malignancy probability.

Our findings align with prior reports demonstrating high diagnostic yields for CT-guided TCNB [1,15]. Whereas earlier studies emphasized lesion size, location,

and operator experience as predictors of diagnostic success, our results highlight the additional value of quantitative HU measurements. By integrating ΔHU analysis, interventional radiologists may obtain an objective assessment of tissue characteristics that extends beyond conventional planning.

To our knowledge, no previous study has systematically quantified HU variation before and after CT-guided transthoracic biopsy in relation to histopathological outcomes. Existing reports have mainly focused on attenuation as a marker of procedural complications rather than diagnostic yield. Zhou *et al*. [16] reported a nonlinear association between lung needle path CT attenuation and immediate pneumothorax risk, with lower HU values associated with higher complication rates. Although these studies focused primarily on complications rather than histopathology, they underscore the relevance of tissue attenuation as a marker of local tissue properties. Despite this potential, no previous studies have specifically examined changes in needle tract attenuation as a predictor of biopsy success in pulmonary nodules.

The strong discriminative performance of ΔHU suggests that these attenuation changes reflect intrinsic tissue characteristics, such as viability and vascularity, rather than being mere procedural observations. While these biological interpretations remain speculative and require confirmation through direct pathological or perfusion imaging correlation, the observed diagnostic accuracy is promising. As our study included a single-center cohort, these findings have not yet been externally validated. However, we utilized predefined imaging variables and standardized measurement and analysis techniques to reduce potential overfitting. Future multicenter studies are warranted to confirm the generalizability of ΔHU as a diagnostic biomarker.

The integration of pre-procedural PET-CT or contrast-enhanced MRI further strengthens the clinical applicability of our findings. Prior work has shown that PET/CT fusion imaging combined with intra-procedural CT can significantly improve diagnostic yield, particularly in heterogeneous or metabolically active lesions [15,17]. In our cohort, PET-CT or MRI-guided targeting likely enhanced the detection of viable, vascularized regions, which corresponded with higher ΔHU values observed in malignant lesions. Notably, small cell carcinoma and adenocarcinoma subtypes exhibited the highest ΔHU, suggesting that increased cellularity or perfusion may contribute to post-biopsy attenuation changes, although inter-subtype differences were not statistically significant.

Age distribution differed significantly among the diagnostic groups, with patients in the malignancy group being older on average than those in the inflammatory group. This finding may reflect the epidemiological tendency for malignancy to occur at older ages, whereas inflammatory or necrotic lesions can present across a wider age range. While gender distribution did not differ significantly among groups, awareness of these demographic patterns may aid clinicians in interpreting biopsy results in the context of patient characteristics.

Laboratory parameters, including hemoglobin, platelet count, INR, PT, and aPTT, were largely within normal limits across all histopathological groups, reflecting careful pre-procedural patient assessment. The absence of significant differences among groups suggests that ΔHU variations are primarily attributable to intrinsic tissue characteristics rather than coagulation abnormalities. Complication rates were consistent with the literature, with pneumothorax and hemorrhage being the most common adverse events [13]. Importantly, complication frequencies did not differ significantly among histopathological categories or malignancy subtypes, supporting the overall safety of CT-guided TCNB when standard precautions are observed.

Although the concept of ΔHU as a marker of tissue viability and vascularity has not been directly validated previously, our study demonstrates its potential incremental value by quantitatively distinguishing malignant from necrotic or inflammatory lesions. These findings suggest that ΔHU may provide complementary information to conventional imaging and help guide more accurate sampling during CT-guided biopsy. From a physiological standpoint, the observed ΔHU differences may be related to tissue perfusion or micro-hemorrhage. While direct perfusion measurements were not performed, these hypothetical interpretations are supported by studies demonstrating correlations between CT perfusion/DCE parameters and microvessel density, attenuation thresholds predictive of necrosis, and characteristic HU evolution in hemorrhage [9–11]. Literature evidence indicating a correlation between perfusion parameters and HU dynamics suggests that ΔHU can serve as an indirect marker of tissue vascularity and viability. Future studies incorporating quantitative perfusion imaging could further validate this mechanistic link.

Clinically, the combination of ΔHU measurement and careful pre-procedural planning offers several advantages. Quantitative HU assessment may help refine target selection, provide immediate feedback on sampling adequacy, and reduce non-diagnostic biopsy rates in heterogeneous lesions containing necrosis or fibrosis. Wider adoption of ΔHU measurement could streamline workflow, minimize repeat procedures, and support decision-making in centers without on-site cytopathology. While PET-CT or MRI guidance may improve lesion targeting and ΔHU assessment, the added cost and workflow implications should be considered. In routine practice, ΔHU measurement using standard CT alone could provide a cost-effective adjunct in centers without advanced imaging resources. When integrated with standard laboratory assessment and procedural precautions, ΔHU may serve as an adjunctive biomarker with the potential to optimize diagnostic yield and procedural safety.

Limitations of this study include the single-center design and relatively small sample sizes in certain histological subgroups, which may limit generalizability and reduce statistical power, particularly for analyses of less common tumor types or histopathological subgroups. Manual ROI placement for HU measurement, though performed independently by two experienced radiologists, introduces potential observer variability. The potential role of automated or semi-automated HU measurement tools could not only reduce interobserver variability but also streamline workflow and enhance real-time biopsy guidance. Future validation studies are warranted to assess the accuracy and clinical utility of such tools. Additionally, subtle micro-air or hemorrhagic changes may still influence HU measurements despite the exclusion of overt artifacts. Finally, variability in the timing of post-biopsy CT acquisition could affect ΔHU, suggesting that standardized post-procedure imaging protocols are warranted.

5. Conclusion

Our study demonstrates that ΔHU measured during CT-guided TCNB is a reliable imaging biomarker of tissue viability and histopathological outcome in thoracic lesions. When combined with careful laboratory evaluation and advanced imaging guidance, ΔHU analysis has the potential to enhance diagnostic accuracy, optimize biopsy targeting and improve patient management in interventional radiology practice.

Key Points

• ΔHU (attenuation change from pre- to post-biopsy) is a novel quantitative biomarker obtained during CT-guided transthoracic core needle biopsy and has not been previously evaluated in thoracic lesions.

• Malignant lesions show a characteristic positive ΔHU, reflecting higher tissue viability/vascularity, whereas inflammatory and necrotic lesions demonstrate minimal or negative ΔHU, respectively, indicating poor perfusion or non-viable tissue.

• ΔHU demonstrated excellent diagnostic accuracy for malignancy (AUC = 0.956), with 94% sensitivity and 78% specificity, outperforming static HU values alone.

• HU measurement during routine pre- and post-biopsy scans is highly reproducible (interobserver α = 0.849), requiring no protocol changes or contrast administration.

• Dynamic HU analysis may improve biopsy targeting, reduce sampling errors in heterogeneous lesions, and increase diagnostic confidence, especially when necrosis or non-diagnostic tissue is a concern.

• Integration of ΔHU into the standard TCNB workflow is feasible, low-cost, and provides immediate real-time quantitative feedback.

Availability of Data and Materials

The data that support the findings of this study are available from the corresponding author upon reasonable request.

Author Contributions

MY, FAY and ÖK designed the research study and wrote the first draft. MY, BK and FAL performed the research. MY, AA and AK analysed the data. All authors contributed to the important editorial changes in the manuscript. All authors read and approved the final manuscript. All authors have participated sufficiently in the work and agreed to be accountable for all aspects of the work.

Ethics Approval and Consent to Participate

The study was approved by the local ethics committee of Atatürk University (approval no: 26, meeting no: 10, date: 28.11.2025) and conducted in accordance with the Declaration of Helsinki. Ethics approval was obtained prior to data analysis and manuscript preparation. Written informed consent for the biopsy procedure was obtained from all patients as part of routine clinical care. Due to the retrospective nature of the study and the use of anonymized data, the requirement for additional research-specific informed consent was waived by the ethics committee.

Acknowledgment

Not applicable.

Funding

This research received no external funding.

Conflict of Interest

The authors declare no conflict of interest.

References

[1] Constantinescu A, Stoicescu ER, Iacob R, Chira CA, Cocolea DM, Nicola AC, *et al*. CT-Guided Transthoracic Core-Needle Biopsy of Pulmonary Nodules: Current Practices, Efficacy, and Safety Considerations. Journal of Clinical Medicine. 2024; 13: 7330. https://doi.org/10.3390/jcm13237330.

[2] Tipaldi MA, Ronconi E, Krokidis ME, Zolovkins A, Orgera G, Laurino F, *et al*. Diagnostic yield of CT-guided lung biopsies: how can we limit negative sampling? The British Journal of Radiology. 2022; 95: 20210434. https://doi.org/10.1259/bjr.20210434.

[3] Wu CC, Maher MM, Shepard JAO. Complications of CT-guided percutaneous needle biopsy of the chest: prevention and management. AJR. American Journal of Roentgenology. 2011; 196: W678–W682. https://doi.org/10.2214/AJR.10.4659.

[4] Chae KJ, Hong H, Yoon SH, Hahn S, Jin GY, Park CM, *et al*. Non-diagnostic Results of Percutaneous Transthoracic Needle Biopsy: A Meta-analysis. Scientific Reports. 2019; 9: 12428. https://doi.org/10.1038/s41598-019-48805-x.

[5] Saggiante L, Biondetti P, Lanza C, Carriero S, Ascenti V, Piacentino F, *et al*. Computed-Tomography-Guided Lung Biopsy:

A Practice-Oriented Document on Techniques and Principles and a Review of the Literature. Diagnostics. 2024; 14: 1089. https://doi.org/10.3390/diagnostics14111089.

[6] Basiri R, Sharifnezhad F, Jafarian AH, Samadi S, Zarghi A. Diagnostic accuracy of percutaneous transthoracic needle biopsy among peripheral pulmonary lesions: a multicenter observational study. Annals of Medicine and Surgery (2012). 2024; 86: 5762–5766. https://doi.org/10.1097/MS9.0000000000002539.

[7] DenOtter TD, Schubert J. Hounsfield Unit. StatPearls. StatPearls Publishing: Treasure Island (FL). 2023.

[8] Tatsugami F, Higaki T, Nakamura Y, Honda Y, Awai K. Dual-energy CT: minimal essentials for radiologists. Japanese Journal of Radiology. 2022; 40: 547–559. https://doi.org/10.1007/s11604-021-01233-2.

[9] Drljevic-Nielsen A, Rasmussen F, Nielsen PS, Stilling C, Thorup K, Mains JR, *et al*. Prognostic value of DCE-CT-derived blood volume and flow compared to core biopsy microvessel density in patients with metastatic renal cell carcinoma. European Radiology Experimental. 2021; 5: 32. https://doi.org/10.1186/s41747-021-00232-2.

[10] Hillal A, Ullberg T, Ramgren B, Wassélius J. Computed tomography in acute intracerebral hemorrhage: neuroimaging predictors of hematoma expansion and outcome. Insights into Imaging. 2022; 13: 180. https://doi.org/10.1186/s13244-022-01309-1.

[11] Arslanoglu A, Chalian H, Sodagari F, Seyal AR, Töre HG, Salem R, *et al*. Threshold for Enhancement in Treated Hepatocellular Carcinoma on MDCT: Effect on Necrosis Quantification. AJR. American Journal of Roentgenology. 2016; 206: 536–543. https://doi.org/10.2214/AJR.15.15339.

[12] Pang G, Shao C, Lv Y, Zhao F. Tumor attenuation and quantitative analysis of perfusion parameters derived from tri-phasic CT scans in hepatocellular carcinoma: Relationship with histological grade. Medicine. 2021; 100: e25627. https://doi.org/10.1097/MD.0000000000025627.

[13] Heerink WJ, de Bock GH, de Jonge GJ, Groen HJM, Vliegenthart R, Oudkerk M. Complication rates of CT-guided transthoracic lung biopsy: meta-analysis. European Radiology. 2017; 27: 138–148. https://doi.org/10.1007/s00330-016-4357-8.

[14] Yazici MM, Sekmen S, Çelik A, Yavaşi Ö, Hürsoy N. The accuracy of the Hounsfield unit in pulmonary embolism diagnostics. Clinical and Experimental Emergency Medicine. 2024; 11: 295–303. https://doi.org/10.15441/ceem.23.113.

[15] Lin Y, Xu Y, Lin J, Fu L, Sun H, Huang Z, *et al*. Improving CT-guided transthoracic biopsy diagnostic yield of lung masses using intraprocedural CT and prior PET/CT fusion imaging. BMC Pulmonary Medicine. 2022; 22: 311. https://doi.org/10.1186/s12890-022-02108-6.

[16] Zhou SQ, Luo F, Ran X, Yang J, Lv FR, Li K. Nonlinear association between lung needle path CT attenuation values and postprocedural immediate pneumothorax following computed tomography-guided lung biopsy: a retrospective cohort study. BMC Pulmonary Medicine. 2024; 24: 567. https://doi.org/10.1186/s12890-024-03343-9.

[17] Malik D, Pant V, Sen I, Thakral P, Das SS, Cb V. The Role of PET-CT-Guided Metabolic Biopsies in Improving Yield of Inconclusive Anatomical Biopsies: A Review of 5 Years in a Teaching Hospital. Diagnostics. 2023; 13: 2221. https://doi.org/10.3390/diagnostics13132221.